PROCEEDINGS OF SCIENCE

Observation of gamma rays from the northern celestial sky up to the sub-PeV range with the Tibet air shower array and its underground muon detector array

S. Kato[a,*] **for the Tibet ASγ collaboration**

[a] *Institute for Cosmic Ray Research, University of Tokyo, Kashiwa, Chiba 277-8582, Japan*

Gamma-ray observation in the sub-PeV range helps us search for Galactic PeV cosmic-ray accelerators, PeVatrons. Measurement of the energy spectrum of gamma rays from astrophysical sources is especially crucial to discuss their hadronic or leptonic origin. In this study, gamma rays from the sky region of HESS J1843−033 are observed by the Tibet air shower array equipped with the underground muon detector array. A new gamma-ray source TASG J1844−038 is detected above 25 TeV with a 6.2 σ level in the region of interest, the position of which is consistent with HESS J1843−033, eHWC J1842−035, and LHAASO J1843−0338. The gamma-ray energy spectrum of TASG J1844−038 is successfully measured in 25−130 TeV for the first time; it smoothly connects to that of HESS J1843−033 and gives consistent flux levels with those of eHWC J1842−035 and LHAASO J1843−0338 at 56 and 100 TeV, respectively. The analysis of the combined gamma-ray spectra between the H.E.S.S., LHAASO, and TASG sources indicates the cutoff at about 50 TeV. The distribution of the molecular clouds around TASG J1844−038 is investigated by analyzing public CO line-emission data; our study finds the clouds in the velocity range of 75−95 km s^{-1} lying flat over the region with a 50 K km s^{-1} level. The association of the observed gamma rays with a nearby supernova remnant SNR G28.6−0.1 is discussed, and it is proposed that cosmic rays accelerated by SNR G28.6−0.1 up to about 500 TeV generate the observed gamma rays from the collisions with the ambient gas found in the analysis.

38th International Cosmic Ray Conference (ICRC2023)
26 July - 3 August, 2023
Nagoya, Japan

*Speaker

© Copyright owned by the author(s) under the terms of the Creative Commons Attribution-NonCommercial-NoDerivatives 4.0 International License (CC BY-NC-ND 4.0).

PoS(ICRC2023)627

1. Introduction

Origin of cosmic rays in the knee region of the energy spectrum has been searched for through gamma-ray observation above 100 TeV (sub-PeV range). Currently, many sub-PeV gamma-ray sources have been detected mainly in the northern sky [1–5]. While it is revealed that supernova remnants, pulsar wind nebulae, and star forming regions are found to be promissing candidates of PeV cosmic-ray accelerators called PeVatrons, still large amount of gamma-ray sources remains unidentified [5, 6]: there is no likely counterpart for the sub-PeV sources. It is worth noting that many of these unidentified sources are not fully investigated to interpret gamma-ray emission mechanism and more observational studies is needed to provide further information on the sources.

This study focuses on the gamma-ray observation of the sky region around HESS J1843-033, an unidentified gamma-ray source found by the H.E.S.S. Galactic Plane Survey [6]. It has, in its vicinity, several SNR candidates [7, 8] and PSR J1844-0346 [9] as well as gamma-ray sources eHWC J1842-035 and LHAASO J1843-0338 [2, 4], but their associations are not detailedly discussed. In particular, the energy spectrum of gamma rays from this sky region is not measured systematically above 30 TeV, which cannot be covered by H.E.S.S., and makes it difficult to interpret the relation between the above sources. The fraction of hadronic contribution to the observed gamma rays from the source has not been constrained from the neutrino observations [10]. This study aims to observe gamma rays from the sky region of HESS J1843-033 by the Tibet air shower array equipped with the underground muon detector array and to discuss its origin.

2. Experiment and Data Analysis

The Tibet air shower array is a cosmic-ray observatory operating since 1991 at Yangbajing (90.522° E, 30.102° N, 4, 300 m a.s.l.), Tibet, China [11–13]. The surface air shower array covers an geometrical area of $65,700\,\mathrm{m}^2$ with 597 plastic scintillation detectors of a $0.5\,\mathrm{m}^2$ area and determines the energies and incoming directions of primary cosmic and gamma rays by detecting particles in extensive air showers [14, 15]. The array of water-Cherenkov-type muon detectors (MDs) with a total geometrical area of $3,400\,\mathrm{m}^2$ is also installed under the ground [1]. The detectors contain a water layer with a 1.5 m depth and detect Cherenkov light emitted by shower muons passing the water. The MD array effectively discriminates primary cosmic and gamma rays and provides high sensitivity to gamma rays from astrophysical sources [16], which has been proved in previous studies [1, 3, 17, 18].

This study uses the data taken by the Tibet air shower array and the MD array from February 2014 to May 2017 (719 live days in total). The data are selected with the criteria introduced by Amenomori et al. (2019) [1] with some following exceptions. First, the zenith-angle range analyzed is extended up to 50° to improve statistics of gamma rays from the HESS J1843-033 region. This extension is effective above 25 TeV from our simulation studies, so the threshold energy is according fixed at 25 TeV. Second, the selection using ΣN_μ, the total number of muons recorded with the MD array (MD cut), is optimized for this study; it requires events to satisfy $\Sigma N_\mu < 1.8\times10^{-3}\left(\Sigma\rho/\mathrm{m}^{-2}\right)$ or $\Sigma N_\mu < 0.4$ where $\Sigma\rho$ is the sum of the particle number density recorded with the surface scintillation detectors. This cut can reduce the background cosmic-ray events to less than a 0.1%

PoS(ICRC2023)627

level while keeping about 80% of gamma-ray events above the gamma-ray equivalent energy of 100 TeV.

Our Monte Carlo (MC) simulation generates a total number of 1.1×10^8 gamma rays following a power-law spectrum with an index of 2.0 using Corsika v7.4000 [19]. These primary events are injected into the atmosphere from a hypothetical point source with a declination of 0° and the developement of air showers are simulated. The detector response for the showers is simulated with Geant4 v10.0 [20]. The simulation includes the calculation of the energy loss of particles in the scintillators and the soil layer and Cherenkov-photon emission in the water layer of MDs. Based on the MC data analysis, the energy and angular resolutions of the experiment are estimated at $\simeq$ 30% and 0.28° (50% containment), respectively.

3. Results

The study defines a square region of interest (ROI) of a $4^\circ \times 4^\circ$ size centered at $(\alpha, \delta) = (281.0^\circ, -3.5^\circ)$ (J2000) which includes HESS J1843-033. The distribution of events is modeled with a source component of an axisymmetric Gaussian plus the background component constructed from the data in OFF regions. Based on a two-dimensional unbinned maximum likelihood analysis, the center of a potential source is determined as $(\alpha, \delta) = (281.09^\circ \pm 0.10^\circ, -3.76^\circ \pm 0.09^\circ)$. The number of events in the circular ON-source window with a radius of 0.7° centered at the determined center is counted, and the number of background is calculated using 20 OFF regions opened following the equi-zenith-angle method [21]. The excess of events in the ON-source window over background is significant with a $6.2\,\sigma$ level [22], leading to a successful detection of a gamma-ray source, which is named TASG J1844-038. Figure 1 shows the significance map of the ROI, in which the position and the extension of TASG J1844-038 as well as those of nearby sources are indicated. The extension of the TASG source is estimated by fitting a one-dimensional Gaussian function to the radial profile of the events against the position of the source, which leads to $0.34^\circ \pm 0.12^\circ$. Accounting for the statistical error of the determined position and the pointing systematics of the experiment [13], the position of TASG J1844-038 is consistent with HESS J1843-033 and the other nearby gamma-ray sources eHWC J1842-035 and LHAASO J1843-0338. The extension of TASG J1844-038 is also consistent with HESS J1843-033 ($0.24^\circ \pm 0.06^\circ$ above $E > 400$ GeV) and eHWC J1842-035 ($0.39^\circ \pm 0.09^\circ$ above $E > 56$ TeV).

Figure 2 shows the energy spectrum of TASG J1844-038 measured between 25 and 130 TeV with the spectra of nearby gamma-ray sources. The energy flux in each bin is calculated only if the gamma-ray detection significance exceeds a $2\,\sigma$ level; otherwise, the 95% upper limit is calculated. The resultant spectrum can be fitted with a simple power-law (PL) function, giving $\mathrm{d}N/\mathrm{d}E = (9.70 \pm 1.89) \times 10^{-16} (E/40\,\mathrm{TeV})^{-3.26\pm0.30}$ TeV^{-1} cm^{-2} s^{-1} with $\chi^2/\mathrm{d.o.f.} = 2.1/2$. The absolute energy scale uncertainty of 12% [13] and the statistical uncertainty in the source extension contribute to the systematic uncertainty in the flux normalization of 43%. It is worth noting that the spectrum of TASG J1844-038 smoothly connects to that of HESS J1843-033 at 30 TeV and also gives consistent energy-flux level with LHAASO J1843-0338 at 100 TeV. The above facts imply the common origin for their gamma-ray emissions, thus favoring the characterization of the combined spectrum of gamma rays from the sky region including the TASG, H.E.S.S., and LHAASO sources. The combined spectra rules out the fit with a simple PL function at a $5\,\sigma$ level ($\chi^2/\mathrm{d.o.f.} = 47.3/9$),

PoS(ICRC2023)627

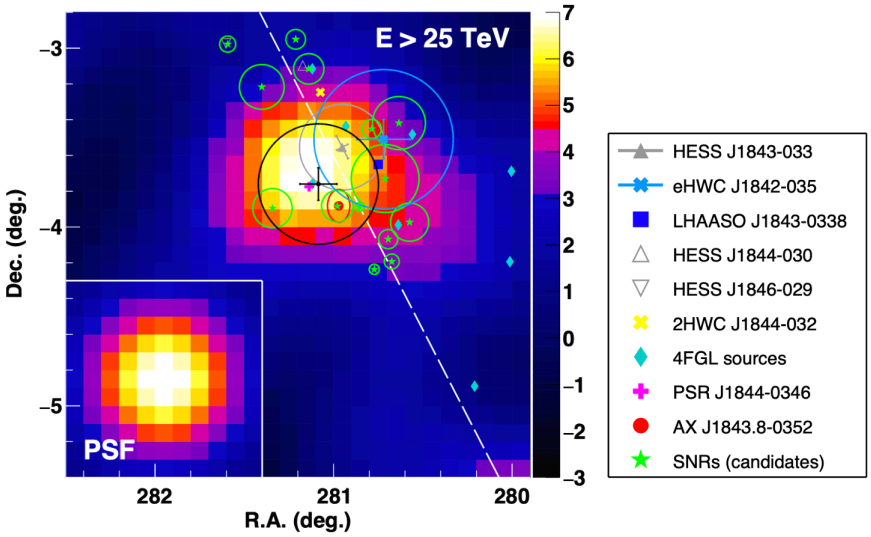

Figure 1: Significance map of the ROI smoothed with the point-spread-function (PSF) radius of the experiment. The position with the statistical errors of TASG J1844-038 is shown with the black cross and the extension with the black circle. The white dashed line shows the Galactic Plane. The symbols and the circles with different colors indicate the positions and the extensions of nearby celestial sources shown in the right legend. The lower-left inset shows the PSF.

and is well expressed with the PL function with exponential cutoff (χ^2/d.o.f. = 10.4/8)

$$\frac{\mathrm{d}N}{\mathrm{d}E} = N_0 \left(\frac{E}{\mathrm{TeV}}\right)^{-\Gamma} \exp\left(-\frac{E}{E_{\mathrm{cut}}}\right) \mathrm{TeV}^{-1}\,\mathrm{cm}^{-2}\,\mathrm{s}^{-1} \tag{1}$$

with the best-fit values of $N_0 = (3.57 \pm 0.26) \times 10^{-16}\,\mathrm{TeV}^{-1}\,\mathrm{cm}^{-2}\,\mathrm{s}^{-1}$, $\Gamma = -2.02 \pm 0.06$, and $E_{\mathrm{cut}} = 49.5 \pm 9.0\,\mathrm{TeV}$.

The highest energy of the observed gamma-ray like events reaches 586 TeV, which is not registered as one of the Galactic diffuse gamma-ray events detected by the Tibet air shower array [18]. It comes from the direction 0.53° apart from the center of TASG J1844-038, but it is not inconsistent to consider that the gamma-ray event is of the TASG J1844-038 origin, taking into account the extension of the source and the experiment's angular resolusion of $\simeq 0.2°$ with a 50% containment. The gamma-ray likeliness of the event is estimated based on the method described in [1] from the number of muons in the shower event detected with the MD array, and the probability of the event being a background cosmic-ray event is calculated as 10^{-4}, highly favoring gamma-ray nature of the event. Therefore, this is the highest energy gamma-ray event observed ever from the direction of HESS J1843-033. On the other hand, the number of Galactic diffuse gamma-ray events is expected to be $\simeq 0.01$, so the scenario that the event is of Galactic diffuse gamma-ray origin cannot be ruled out (only disfavored with $2.3\,\sigma$ assuming the Poisson statistics).

4. Discussion

In this section, the associations of the observed gamma rays with SNR G28.6-0.1 and PSR J1844-0346, which are located within a positional uncertainty of TASG J1844-038, are discussed.

PoS(ICRC2023)627

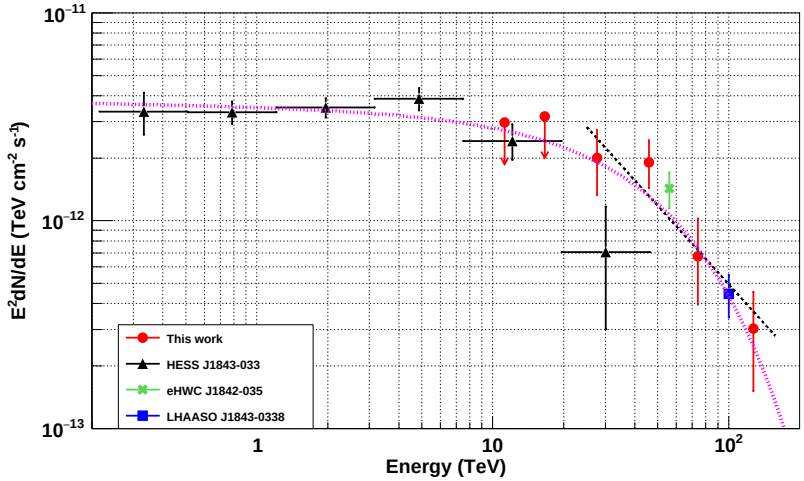

Figure 2: Energy spectra of TASG J1844-038 (red) and nearby gamma-ray sources [2, 4, 6]. The error bars are statistical and the downward arrows indicate the 95% upper limits. The black dotted line is the best-fit PL function to our result, and the magenta short-dotted curve is the best-fit ECPL function (1) to the combined spectra between HESS, LHAASO, and this work. The figure is cited from Amenomori et al. (2022) [23]. The flux of eHWC J1842-035 is our calculation from the published integral flux above 56 TeV [2].

Association with SNR G28.6-0.1 SNR G28.6-0.1 has a complex morphology seen in radio (G28.60-0.13) found by Helfand et al. (1989) [24]. Later, the observation by the X-ray satellite ASCA detected an X-ray source ASCA J1843.8-0352 overlapping with the radio complex, and the authors concluded that the ASCA source is a supernova remnant with an age less than 2.7 kyr in which high-energy electrons are accelerated [7]. Ueno et al. (2003) estimated the magnetic field in the remnant at $\sim 6\,\mu$G and the maximum acceleration energy of the electrons at ~ 200 TeV [25]. In the above relatively weak magnetic-field strength, the energies of parent electrons for the observed non-thermal keV X-rays and gamma rays with $E \lesssim 100$ TeV generated through Inverse Compton Scattering (ICS) should be the same order, thus leading to the same extensions of the X- and gamma-ray emissions. However, there is a possible discrepancy of a $2.3\,\sigma$ level between the extensions of TASG J1844-038 ($0.34^\circ \pm 0.12^\circ$) and of ASCA J1843.8-0352 (average radius of $4.5'$ [25]), which indicates a hadronic contribution to the observed gamma rays. Under such a situation, the cutoff in the energy spectrum of the contributing cosmic-ray protons would be at ~ 500 TeV, roughly one order of magnitude higher than the cutoff of $\simeq 50$ TeV in the gamma-ray energy spectrum, as found from our combined fit.

To validate the above idea, the distribution of target materials for cosmic rays to produce π^0-decay gamma rays, such as molecular clouds, should be investigated. Ranasinghe & Leahy (2018) determined the distance to the SNR as 9.6 kpc by measuring the HI absorption spectra and detecting molecular clouds geometrically associated with the SNR in the velocity range of $\simeq 86\,\mathrm{km\,s^{-1}}$ [26]. Considering the previous study, the ^{12}CO ($J = 1 - 0$) line emission data published by the FUGIN Galactic Plane survey [27] are analyzed in the velocity range of $75 - 95\,\mathrm{km\,s^{-1}}$ and the distribution of molecular clouds is compared with the position of TASG J1844-038. The result shown in Figure 3 tells us that diffuse clouds lie flat over the TASG source extension with a $\sim 50\,\mathrm{K\,km\,s^{-1}}$ level.

PoS(ICRC2023)627

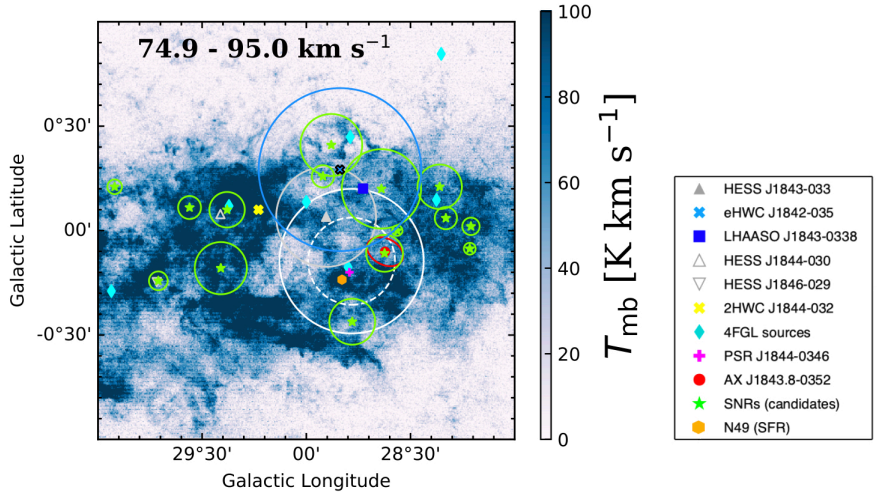

Figure 3: Brightness-temperature map of the ^{12}CO ($J = 1 - 0$) line emission. The position uncertainty and the extension of TASG J1844-038 are shown by the white dashed and solid lines, respectively. The positions and extensions of nearby celestial sources are shown with symbols and circles with different colors, respectively. The figure is cited from Amenomori et al. (2022) [23].

Therefore, it would be adequate to consider that cosmic-ray protons are possibly accelerated up to $\sim$ 500 TeV by SNR G28.6-0.1 and diffuse into the molecular clouds producing π^0-decay gamma rays from the collisions.

Association with PSR J1844-0346 A gamma-ray PSR J1844-0346 (also named 4FGL J1844.4–0345 [28]), discovered by the Fermi-LAT gamma-ray telescope [9], is another candidate for the counterpart of TASG J1844-038. Its spin period, spin-down luminosity, and characteristic age are $P = 113$ ms, $\dot{E} = 4.2 \times 10^{36}$ erg s^{-1}, $\tau_c = 12$ kyr respectively. It is noteworthy to associate the TeV gamma-ray emission of HESS J1843-033 with PSR J1844-0346. Assuming the pulsar's distance of 4.3 kpc for HESS J1843-033 [29], the TeV gamma-ray flux of 1.1×10^{-11} erg cm^{-2} s^{-1} corresponds to the luminosity of $2.4 \simeq 10^{34}$ erg s^{-1} and the extension of 0.24° translates into the physical size of $\simeq$ 18 pc [6]. These characteristics of TeV gamma rays are typical for TeV pulsar wind nebulae [30]. Therefore, the gamma rays from TASG J1844-038, whose spectrum is continuously connected from that of HESS J1843-033, can be associated with the PSR J1844-0346 under the leptonic scenario: gamma rays are produced from ICS off the cosmic microwave background radiation by high energy electrons accelerated in the pulsar-wind nebula around the PSR. In this scenario, our spectral analysis indicates the maximum acceleration energy for electrons of $\simeq$ 100 TeV. If the magnetic-field strength of 3 μG is assumed, the cooling time of electrons due to the synchrotron emission and ICS is roughly $\sim$ 10 kyr [31], which is similar to τ_c of the PSR. The diffusion coefficient D of $\sim$ 100 TeV electrons can be roughly estimated with $2\sqrt{Dt_{\rm cool}} = R_{\rm ext}$ [32], where $t_{\rm cool}$ is the cooling time estimated above, and $R_{\rm ext}$ the extension of TASG J1844-038 (0.34° in apparent radius and thus $\simeq$ 26 pc at the distance of 4.3 kpc). The estimation results in $D \sim 5 \times 10^{27}$ cm^2 s^{-1} implying that the particle diffusion is suppressed more than two orders of magnitude than the Galactic average [33]. The suppression is also observed for the Geminga PWN by HAWC [34] which is recently studied as a category of celestial objects called *TeV halo* [35]. No PWN-like radio nor X-ray emission is

PoS(ICRC2023)627

found around PSR J1844-0346 [36], which is consistent with the typical nature of TeV halos. Some theoretical studies also propose the suppression of particle diffusion in halos by about two orders of magnitude [37, 38].

5. Conclusions

Data taken by the Tibet air shower array and the MD array are analyzed to study gamma rays from the sky region of HESS J1843-033. A new gamma-ray source TASG J1844-038 is detected with a $6.2\,\sigma$ level and its position is consistent with nearby gamma-ray sources. The extension is estimated at $0.34^\circ \pm 0.12^\circ$, also consistent with those of the HESS J1843-033 and eHWC J1842-035. The energy spectrum is measured between 25 and 130 TeV and can be fitted with a simple PL function of $\mathrm{d}N/\mathrm{d}E = (9.70 \pm 1.89) \times 10^{-16}(E/40\,\mathrm{TeV})^{-3.26\pm0.30}\,\mathrm{TeV}^{-1}\,\mathrm{cm}^{-2}\,\mathrm{s}^{-1}$. The fit of a PL function with an exponential cutoff to the combined spectra between TASG J1844-038, HESS J1843-033, and LHAASO J1843-0338 results in a cutoff energy of 49.5 ± 9.0 TeV. Discussions of the associations of TASG J1844-038 both with SNR G28.6-0.1 and PSR J1844-0346 lead to fascinating scenarios: cosmic-ray proton acceleration in SNR G28.6-0.1 up to ~ 500 TeV and the slow diffusion of high-energy electrons with energies up to $\simeq 100$ TeV in a TeV halo produced by PSR J1844-0346. However, our simple discussion cannot account for the complex morphology of HESS J1843-033, which may require detailed theoretical modeling. In addition, the associations of the observed gamma-ray emission with other nearby SNR candidates [8] and the star forming region N49 [39] (see Figure 3) should also be study in the future.

Acknowledgments

The collaborative experiment of the Tibet Air Shower Arrays has been conducted under the auspices of the Ministry of Science and Technology of China and the Ministry of Foreign Affairs of Japan. This work was supported in part by a Grant-in-Aid for Scientific Research on Priority Areas from the Ministry of Education, Culture, Sports, Science and Technology, and by Grants-in-Aid for Science Research from the Japan Society for the Promotion of Science in Japan. This work is supported by the National Natural Science Foundation of China under Grants No. 12227804, No. 12275282, No. 12103056 and No. 12073050, and the Key Laboratory of Particle Astrophysics, Institute of High Energy Physics, CAS. This work is also supported by the joint research program of the Institute for Cosmic Ray Research (ICRR), the University of Tokyo. This publication makes use of data from FUGIN, FOREST Unbiased Galactic plane Imaging survey with the Nobeyama 45-m telescope, a legacy project in the Nobeyama 45-m radio telescope. Nobeyama Radio Observatory is a branch of the National Astronomical Observatory of Japan, National Institutes of Natural Sciences. S. Kato appreciates the support from JST SPRING, Grant Number JPMJSP2108.

References

[1] M. Amenomori et al. *Phys. Rev. Lett.*, 123:051101, Jul 2019.
[2] A. U. Abeysekara et al. *Phys. Rev. Lett.*, 124:021102, Jan 2020.
[3] M. Amenomori et al. *Nature Astronomy*, 5:460, 2021.
[4] Z. Cao et al. *Nature*, 594:33, 2021.

PoS(ICRC2023)627

[5] Z. Cao et al. *arXiv:2305.17030v1*.
[6] H.E.S.S. collaboration. *Astronomy & Astrophysics*, 612:A1, 2018.
[7] A. Bamba et al. *Publications of the Astronomical Society of Japan*, 53:L21, 2001.
[8] L. D. Anderson et al. *A&A*, 605:A58, 2017.
[9] C. J. Clark et al. *The Astrophysical Journal*, 834(2):106, jan 2017.
[10] T. Q. Huang and Z. Li. *The Astrophysical Journal*, 925:85, 2022.
[11] M. Amenomori et al. *Phys. Rev. Lett.*, 69:2468–2471, Oct 1992.
[12] M. Amenomori et al. *The Astrophysical Journal*, 525(2):L93–L96, nov 1999.
[13] M. Amenomori et al. *The Astrophysical Journal*, 692(1):61–72, feb 2009.
[14] M. Amenomori et al. *The Astrophysical Journal*, 678(2):1165–1179, may 2008.
[15] K. Kawata et al. *Experimental Astronomy*, 44:1, 2017.
[16] T. K. Sako et al. *Astroparticle Physics*, 32:177, 2009.
[17] M. Amenomori et al. *Phys. Rev. Lett.*, 127:031102, Jul 2021.
[18] M. Amenomori et al. *Phys. Rev. Lett.*, 126:141101, Apr 2021.
[19] D. Heck et al. *FZKA-6019*, 2 1998.
[20] S. Agostinelli et al. *Nuclear Instruments and Methods in Physics Research Section A: Accelerators, Spectrometers, Detectors and Associated Equipment*, 506(3):250–303, 2003.
[21] M. Amenomori et al. *The Astrophysical Journal*, 598(1):242–249, nov 2003.
[22] T-P. Li and Y-Q. Ma. *The Astrophysical Journal*, 272:317, 1983.
[23] M. Amenomori et al. *The Astrophysical Journal*, 932(2):120, jun 2022.
[24] D. J. Helfand et al. *The Astrophysical Journal*, 341:151, 1989.
[25] M. Ueno et al. *The Astrophysical Journal*, 588(1):338–343, may 2003.
[26] S. Ranasinghe and D. A. Leahy. *Monthly Notices of the Royal Astronomical Society*, 477:2243, 2018.
[27] T. Umemoto et al. *Publications of the Astronomical Society of Japan*, 69(5), 08 2017. 78.
[28] S. Abdollahi et al. *The Astrophysical Journal Supplement Series*, 247(1):33, mar 2020.
[29] P. M. Saz Parkinson et al. *The Astrophysical Journal*, 725(1):571, nov 2010.
[30] H.E.S.S. collaboration. *Astronomy & Astrophysics*, 612:A2, 2018.
[31] J. A. Hinton and W. Hofmann. *The Annual Review of Astronomy and Astrophysics*, 47:523, 2009.
[32] F. A. Aharonian and A. M. Atoyan. *A&A*, 309:917–928, 1996.
[33] S. Gabici et al. *Monthly Notices of the Royal Astronomical Society*, 396:1629, 2009.
[34] A. U. Abeysekara et al. *Science*, 358(6365):911–914, 2017.
[35] T. Linden. *PoS*, ICRC2021:931, 2021.
[36] J. Devin et al. *Astronomy & Astrophysics*, 647:68, 2021.
[37] C. Evoli et al. *Phys. Rev. D*, 98:063017, Sep 2018.
[38] P. Mukhopadhyay and T. Linden. *Phys. Rev. D*, 105:123008, Jun 2022.
[39] W. J. Dirienzo et al. *The Astrophysical Journal*, 144:173, 2012.

PoS(ICRC2023)627

Full Authors List: Tibet ASγ Collaboration

M. Amenomori[1], Y. W. Bao[2], X. J. Bi[3], D. Chen[4], T. L. Chen[5], W. Y. Chen[3], Xu Chen[4], Y. Chen[2], Cirennima[5], S. W. Cui[6], Danzengluobu[5], L. K. Ding[3], J. H. Fang[3,7], K. Fang[3], C. F. Feng[8], Zhaoyang Feng[3], Z. Y. Feng[9], Qi Gao[5], Q. B. Gou[3], Y. Q. Guo[3], Y. Y. Guo[3], Y. Hayashi[10], H. H. He[3], Z. T. He[6], K. Hibino[11], N. Hotta[12], Haibing Hu[5], H. B. Hu[3], K. Y. Hu[3,7], J. Huang[3], H. Y. Jia[9], L. Jiang[3], P. Jiang[4], H. B. Jin[4], K. Kasahara[13], Y. Katayose[14], C. Kato[10], S. Kato[15], I. Kawahara[14], T. Kawashima[15], K. Kawata[15], M. Kozai[16], Labaciren[5], G. M. Le[17], A. F. Li[3,9,18], H. J. Li[5], W. J. Li[3,10], Y. Li[4], Y. H. Lin[3,7], B. Liu[19], C. Liu[3], J. S. Liu[3], L. Y. Liu[4], M. Y. Liu[5], W. Liu[3], H. Lu[3], T. Makishima[14], Y. Masuda[10], S. Matsuhashi[14], M. Matsumoto[10], X. R. Meng[5], Y. Meng[3,7], A. Mizuno[15], K. Munakata[10], Y. Nakamura[15], H. Nanjo[1], C. C. Ning[5], M. Nishizawa[20], R. Noguchi[14], M. Ohnishi[15], S. Okukawa[14], S. Ozawa[21], X. Qian[4], X. L. Qian[22], X. B. Qu[23], T. Saito[24], M. Sakata[25], T. Sako[15], T. K. Sako[15], T. Sasaki[11], J. Shao[3,9], T. Shibasaki[26], M. Shibata[14], A. Shiomi[26], H. Sugimoto[27], W. Takano[11], M. Takita[15], Y. H. Tan[3], N. Tateyama[11], S. Torii[28], H. Tsuchiya[29], S. Udo[11], R. Usui[14], H. Wang[3], S. F. Wang[5], Y. P. Wang[5], Wangdui[5], H. R. Wu[3], Q. Wu[5], J. L. Xu[4], L. Xue[8], Z. Yang[3], Y. Q. Yao[4], J. Yin[4], Y. Yokoe[15], Y. L. Yu[3,7], A. F. Yuan[5], L. M. Zhai[4], H. M. Zhang[3], J. L. Zhang[3], X. Zhang[2], X. Y. Zhang[8], Y. Zhang[3], Yi Zhang[30], Ying Zhang[3], S. P. Zhao[3], Zhaxisangzhu[5], X. X. Zhou[9] and Y. H. Zou[3,7]

[1]Department of Physics, Hirosaki University, Hirosaki 036-8561, Japan.
[2]School of Astronomy and Space Science, Nanjing University, Nanjing 210093, China.
[3]Key Laboratory of Particle Astrophysics, Institute of High Energy Physics, Chinese Academy of Sciences, Beijing 100049, China.
[4]National Astronomical Observatories, Chinese Academy of Sciences, Beijing 100101, China.
[5]Department of Mathematics and Physics, Tibet University, Lhasa 850000, China.
[6]Department of Physics, Hebei Normal University, Shijiazhuang 050016, China.
[7]University of Chinese Academy of Sciences, Beijing 100049, China.
[8]Institute of Frontier and Interdisciplinary Science and Key Laboratory of Particle Physics and Particle Irradiation (MOE), Shandong University, Qingdao 266237, China.
[9]Institute of Modern Physics, SouthWest Jiaotong University, Chengdu 610031, China.
[10]Department of Physics, Shinshu University, Matsumoto 390-8621, Japan.
[11]Faculty of Engineering, Kanagawa University, Yokohama 221-8686, Japan.
[12]Faculty of Education, Utsunomiya University, Utsunomiya 321-8505, Japan.
[13]Faculty of Systems Engineering, Shibaura Institute of Technology, Omiya 330-8570, Japan.
[14]Faculty of Engineering, Yokohama National University, Yokohama 240-8501, Japan.
[15]Institute for Cosmic Ray Research, University of Tokyo, Kashiwa 277-8582, Japan.
[16]Polar Environment Data Science Center, Joint Support-Center for Data Science Research, Research Organization of Information and Systems, Tachikawa 190-0014, Japan.
[17]National Center for Space Weather, China Meteorological Administration, Beijing 100081, China.
[18]School of Information Science and Engineering, Shandong Agriculture University, Taian 271018, China.
[19]Department of Astronomy, School of Physical Sciences, University of Science and Technology of China, Hefei 230026, China.
[20]National Institute of Informatics, Tokyo 101-8430, Japan.
[21]National Institute of Information and Communications Technology, Tokyo 184-8795, Japan.
[22]Department of Mechanical and Electrical Engineering, Shangdong Management University, Jinan 250357, China.
[23]College of Science, China University of Petroleum, Qingdao 266555, China.
[24]Tokyo Metropolitan College of Industrial Technology, Tokyo 116-8523, Japan.
[25]Department of Physics, Konan University, Kobe 658-8501, Japan.
[26]College of Industrial Technology, Nihon University, Narashino 275-8575, Japan.
[27]Shonan Institute of Technology, Fujisawa 251-8511, Japan.
[28]Research Institute for Science and Engineering, Waseda University, Tokyo 162-0044, Japan.
[29]Japan Atomic Energy Agency, Tokai-mura 319-1195, Japan.
[30]Key Laboratory of Dark Matter and Space Astronomy, Purple Mountain Observatory, Chinese Academy of Sciences, Nanjing 210034, China.

PoS(ICRC2023)627